Virtual microphone sensing through vibro-acoustic modelling and Kalman filtering

van de Walle, A.

Dept. Mech. Engng, KU Leuven, Celestijnenlaan 300B, B-3001 Heverlee, Belgium

Naets, F.

Dept. Mech. Engng, KU Leuven, Celestijnenlaan 300B, B-3001 Heverlee, Belgium

Desmet, W.

Dept. Mech. Engng, KU Leuven, Celestijnenlaan 300B, B-3001 Heverlee, Belgium

Abstract

The most straightforward way of obtaining the actual sound pressure at a specific location is to directly measure it using a microphone. In practice however, only a limited number of locations can be instrumented, and some locations of interest may be difficult to reach or may prove to be impractical for direct measurements. This paper therefore proposes a virtual sensing approach that combines readily available microphone measurements with a numerical model to provide virtual measurements of the sound pressure at the uninstrumented locations of interest. State of the art numerical modelling and model order reduction techniques are coupled to a Kalman filter to develop a new formalism for virtual microphone sensing. The developed method is able to deal with complex and strongly coupled vibro-acoustic systems while still remaining real-time capable. The proposed approach is

Email address: axel.vandewalle@kuleuven.be (van de Walle, A.)

validated experimentally.

Keywords: Vibro-acoustics, State-estimation, Kalman filtering

1. Introduction

Several approaches exist for obtaining insight in the acoustic characteristics and performance of a product or system. A first possibility is the analysis of experimental data gathered in a measurement campaign. The main advantage of this approach is that experimental measurements reflect the performance of the real system in operating conditions. However, setting up a full measurement campaign can be costly and time-consuming, not all locations of interest are always easily accessible, and the gathered data can be corrupted by measurement noise. While experimental measurements can be used to quantitatively evaluate the acoustic performance of a product, they do not necessarily provide sufficient insight in the underlying sound generating mechanisms. In a different approach, numerical modelling tools are used to analyse the system. While simulations provide clear insight in the underlying physical processes in complex systems, they are often only an approximate representation of what happens in the real system.

The virtual sensing approach presented in this paper attempts to get the best of both worlds by combining high fidelity numerical models with easily (and cheaply) attainable experimental data. Doing so makes it possible to estimate or virtually measure the sound at any desired location, and blends the real-world accuracy of experimental measurements with the insights and flexibility that only numerical models can provide.

Existing work in virtual sensing for (vibro-)acoustics has mainly emerged from active noise control applications [1, 2, 3, 4, 5], where a zone of quiet is generated in a small area around an error microphone. In many situations it is not possible to mount a physical error microphone sufficiently close to the desired location of attenuation (for example in an observer's ear). A possible solution then consists in using a virtual error microphone instead of a physical one for the control action. An overview of virtual sensing algorithms for active noise control can be found in [1]. The Kalman filter emerges as one of the most promising virtual sensing tools, but Moreau *et al.* claim that the main disadvantages of this method are that a preliminary system identification is required to generate a state space model and that it is limited to systems of relatively low order.

Petersen *et al.* implement a Kalman filter approach to virtual sensing on an acoustic duct arrangement and experimentally validate their approach in [3]. While they show the potential of the method, the application only considers a one-dimensional acoustic problem and requires a preliminary identification stage, which both hinder the generalization to larger and more complex systems.

In [4] Halim *et al.* develop a Kalman filter approach to virtual sensing for coupled vibro-acoustic enclosures which relies on structural sensors to generate virtual acoustic measurements. The modal decomposition method [6] is used to generate a state space model, eliminating the need for a system

identification stage and allowing for application to three-dimensional systems. However, this modelling method only employs in-vacuo panel modes and rigid-walled cavity modes to represent the system dynamics, which is a rather crude approach and introduces substantial modelling errors. These will in turn have a negative effect on the real-world performance of the virtual sensing algorithm. Any experimental validation of the developed method is lacking in the paper. It is also worth noting that the use of the modal decomposition method inherently restricts the method to enclosed vibro-acoustic systems.

In this paper a virtual sensing method is proposed that combines a high-fidelity, three-dimensional numerical vibro-acoustic model with a limited number of microphone measurements in a Kalman filter. This new approach overcomes all of the aforementioned problems related to existing virtual sensing methods. A numerical finite element model of the considered vibro-acoustic system is used in order to avoid an experimental system identification stage. The finite element method is widely used in industrial practice and is able to provide accurate numerical models for a broad variety of vibro-acoustic systems. It can deal with both interior and exterior acoustic problems, complex geometries and advanced damping descriptions. The only problem is that it often results in systems of very high order, rendering it practically impossible to use in a Kalman filter. To this end state of the art model order reduction techniques are used to obtain an accurate system representation of very low order. This approach solves both problems Moreau *et al.* list in [1] as being the main shortcomings of the Kalman filter

for virtual sensing. The method proposed in this paper is real-time capable, and is validated experimentally to verify its real-world performance.

The paper is structured as follows: Section 2 reviews the basic concepts of the Kalman filter for virtual sensing. Next, section 3 introduces the numerical models and model order reduction techniques that are used. The influence of the choice of model description and instrumentation on the observability of the system is studied in section 4. Section 5 presents a complete roadmap describing the required steps to create a virtual sensor. Section 6 presents the experimental validation of the proposed method for virtual microphone sensing, and concluding remarks are made in section 7.

2. Kalman filter for virtual sensing

In this work, the Kalman filter forms the basis for the virtual sensor. The Kalman filter is known to be an optimal estimator for linear systems [7]. Even though this is a relatively simple approach, it allows to obtain an effective trade-off between model based predictions and measurements. In this work we use the regular discrete Kalman filter for linear systems. This filter is defined for a discrete-time state-space system:

$$\mathbf{x}_{k+1} = \mathbf{A}^d\mathbf{x}_k + \mathbf{B}^d\mathbf{b}_k + \mathbf{s}_k \tag{1}$$

$$\mathbf{h}_{k+1} = \mathbf{H}\mathbf{x}_{k+1} + \mathbf{r}_{k+1} \tag{2}$$

where

- $\mathbf{x}_k$ is the state-space vector for a given model at time k.
- $\mathbf{A}^d$ is the discrete-time state transition matrix.

- $\mathbf{B}^d$ is the discrete time input matrix.
- $\mathbf{b}_k$ is the external input at time k.
- $\mathbf{s}_k$ is the random model uncertainty at time k with zero mean and covariance $\mathbf{\Sigma}_s$. This uncertainty is caused both by inaccurately modelled effects and by random unknown inputs to the system.
- $\mathbf{h}_k$ is the measurement value obtained at time k
- $\mathbf{H}$ is the measurement matrix which transforms the states into the measurement outputs.
- $\mathbf{r}_k$ is the random measurement uncertainty at time k with zero mean and covariance $\mathbf{\Sigma}_r$. The uncertainty of these measured outputs is caused (among others) by sensor noise and sensor misplacement.

In Sec. 3 we discuss in detail how these discrete state-space model matrices can be defined for a vibro-acoustic system. Starting from this state-space model description of a system, the Kalman filter equations are:

- Prediction step:

$$\mathbf{x}_{k+1} = \mathbf{A}^d\mathbf{x}_k + \mathbf{B}^d\mathbf{b}_k \tag{3}$$

$$\mathbf{P}_{k+1} = \mathbf{A}^d\mathbf{P}_k\left(A^d\right)^T + \mathbf{\Sigma}_s \tag{4}$$

- Kalman gain computation:

$$\mathbf{G}^k = \mathbf{P}_{k+1}\left(\mathbf{H}\right)^T\left(\mathbf{H}\mathbf{P}_{k+1}\left(\mathbf{H}\right)^T + \mathbf{\Sigma}_r\right)^{-1} \tag{5}$$

- Correction step:

$$\mathbf{x}_{k+1} = \mathbf{x}_{k+1} + \mathbf{G}^k \left(\mathbf{h}_{k+1} - \mathbf{H}\mathbf{x}_{k+1}\right) \quad (6)$$

$$\mathbf{P}_{k+1} = \left(\mathbf{I} - \mathbf{G}^k\mathbf{H}\right)\mathbf{P}_{k+1} \quad (7)$$

Practically this approach can only be applied to models of limited size. This is both due to numerical issues with computing the propagation of the covariances and the inverses but also due to the scaling of the computational cost as the number of estimated corvariances increases quadratically with the number of DOFs. Moreover, stability of the underlying model is key for long term estimation. In this work we therefore propose to use a reduced order model of a vibro-acoustic finite element model. The FE model allows to develop virtual sensors for arbitrary geometries easily. In a second stage, the reduced order model allows to limit the number of DOFs while maintaining a desired accuracy in a certain frequency range. However, specific measures are proposed in order to guarantee the stability of the ROM, which is non-trivial for vibro-acoustic models.

3. Reduced vibro-acoustic modelling

Using a physics-based numerical method to generate a state space model for use in the Kalman filter eliminates the need for an experimental system identification stage. Additionally this enables performing a virtual measurement at any desired output location, even when this location is not directly accessible for physical microphone measurements (and thus, not available for experimental system identification).

In order to develop a numerical model that is suitable for use in the Kalman filter, the finite element method is used to spatially discretize the governing equations, resulting in a large system of differential equations. This system of equations can be expressed in matrix form as

$$\mathbf{M}\ddot{\mathbf{d}} + \mathbf{C}\dot{\mathbf{d}} + \mathbf{K}\mathbf{d} = \mathbf{f}, \tag{8}$$

where $\mathbf{M}$, $\mathbf{C}$ and $\mathbf{K} \in \mathbb{C}^{n\times n}$ are the mass, damping and stiffness matrices, $\mathbf{f} \in \mathbb{C}^n$ is the forcing vector and $\mathbf{d} \in \mathbb{C}^n$ is the system state, with n being the number of degrees of freedom (DOF) in the coupled FE model for the vibro-acoustic system.

Approximate the FE DOFs with a low-rank reduced order basis (ROB):

$$\mathbf{d} \approx \mathbf{V}\mathbf{q}, \tag{9}$$

for $\mathbf{V} \in \mathbb{C}^{n\times n_r}$ and $\mathbf{q} \in \mathbb{C}^{n_r}$ and $n_r \ll n$. When employing a symmetric projection [8] the reduced ODE can be written as:

$$\mathbf{M}^r\ddot{\mathbf{q}} + \mathbf{C}^r\dot{\mathbf{q}} + \mathbf{K}^r\mathbf{q} = \mathbf{f}^r, \tag{10}$$

with

$$\begin{aligned} \mathbf{M}^r &= \mathbf{V}^T\mathbf{M}\mathbf{V} \qquad & \mathbf{C}^r &= \mathbf{V}^T\mathbf{C}\mathbf{V} \\ \mathbf{K}^r &= \mathbf{V}^T\mathbf{K}\mathbf{V} \qquad & \mathbf{f}^r &= \mathbf{V}^T\mathbf{f} \end{aligned} \tag{11}$$

The reduced system matrices are of size $n_r \times n_r$ instead of the original $n \times n$.

3.1. Preservation of stability for the reduced order model

As virtual sensing applications inherently require time-domain models, it is essential for the model reduction process to preserve the stability of the

original finite element model. The way in which the vibro-acoustic coupling manifests itself in the system matrices makes this a non-trivial task, as it either results in a loss of symmetry or a loss of positive definiteness. This problem was studied by van de Walle *et al.* [8] where two distinct approaches were proposed to preserve stability under model reduction. The appropriate method depends on the way in which the vibro-acoustic system is formulated, starting from the regular displacement and pressure formulation ($u-p$) or starting from an adjusted FE description ($u-\phi$). We briefly review both approaches in Sec. 3.1.1-3.1.2.

3.1.1. $u-p$ formulation

The most natural way of formulating a coupled vibro-acoustic system in a spatial finite-element framework is by using nodal displacements ($\mathbf{u}$) to describe the structural vibrations and nodal pressures ($\mathbf{p}$) to describe the acoustic domain. This results in the so-called $u-p$ formulation, described by the following ordinary differential equation in time:

$$\mathbf{M}^{up}\ddot{\mathbf{d}}^{up} + \mathbf{C}^{up}\dot{\mathbf{d}}^{up} + \mathbf{K}^{up}\mathbf{d}^{up} = \mathbf{f}^{up}, \tag{12}$$

with

$$\begin{aligned} \mathbf{M}^{up} &= \begin{bmatrix} \mathbf{M}_{uu} & \mathbf{0} \\ -\rho\mathbf{M}_{pu}^{T} & \mathbf{M}_{pp} \end{bmatrix}, \quad \mathbf{C}^{up} = \begin{bmatrix} \mathbf{C}_{uu} & \mathbf{0} \\ \mathbf{0} & \mathbf{C}_{pp} \end{bmatrix}, \\ \mathbf{K}^{up} &= \begin{bmatrix} \mathbf{K}_{uu} & \mathbf{K}_{up} \\ \mathbf{0} & \mathbf{K}_{pp} \end{bmatrix} \end{aligned} \tag{13}$$

and

$$\mathbf{d}^{up} = \begin{bmatrix} \mathbf{u} \\ \mathbf{p} \end{bmatrix}, \qquad \mathbf{f}^{up} = \begin{bmatrix} \mathbf{f}_u \\ \mathbf{f}_p \end{bmatrix}. \tag{14}$$

In order to preserve the stability of the model in this formulation while performing model reduction, we propose to use an extended projection matrix approach [8]. Extending the projection matrix in this way leads to an increase in ROM size, so preservation of stability comes at a cost when using the $u-p$ formulation. The ROM resulting from the extended projection matrix can become up to twice as large as compared to the standard one.

3.1.2. $u-\phi$ formulation

An alternative approach in order to obtain a stable ROM is to reformulate the finite-element system formulation. If chosen well, this allows to use any regular projection matrix in a Galerkin projection [8]. As a consequence there is no increase in ROM size associated with this method. The adapted formulation uses a vector of nodal fluid velocity potentials $\boldsymbol{\phi}$ instead of the pressure $\mathbf{p}$ for describing the acoustic domain. These two quantities are coupled through the relationship:

$$\mathbf{p} = -\rho\dot{\boldsymbol{\phi}}. \tag{15}$$

which then leads to the following spatially discretised vibro-acoustic model in $u-\phi$ formulation :

$$\mathbf{M}^{u\phi}\ddot{\mathbf{d}}^{u\phi} + \mathbf{C}^{u\phi}\dot{\mathbf{d}}^{u\phi} +^{u\phi} \mathbf{d}^{u\phi} = \mathbf{f}^{u\phi}, \tag{16}$$

where the system model matrices can be easily derived from any $u-p$ finite-element model:

$$\begin{aligned} \mathbf{M}^{u\phi} &= \begin{bmatrix} \mathbf{M}_{uu} & \mathbf{0} \\ \mathbf{0} & -\rho\mathbf{M}_{pp} \end{bmatrix}, \quad \mathbf{C}^{u\phi} = \begin{bmatrix} \mathbf{C}_{uu} & -\rho\mathbf{K}_{up} \\ -\rho\mathbf{K}_{up}^T & -\rho\mathbf{C}_{pp} \end{bmatrix}, \\ \mathbf{K}^{u\phi} &= \begin{bmatrix} \mathbf{K}_{uu} & \mathbf{0} \\ \mathbf{0} & -\rho\mathbf{K}_{pp} \end{bmatrix} \end{aligned} \tag{17}$$

and

$$\mathbf{d}^{u\phi} = \begin{bmatrix} \mathbf{u} \\ \boldsymbol{\phi} \end{bmatrix}, \qquad \mathbf{f}^{u\phi} = \begin{bmatrix} \mathbf{f}^{u} \\ -\mathbf{f}^{\phi} \end{bmatrix}. \tag{18}$$

It has to be noted that the formulation proposed by van de Walle *et al.* [8] for the $u-\phi$ formulation differs slightly from the classical description proposed by Everstine *et al.* [9] as the sign of the equations governing the acoustic domain is inverted. This small modification allows to obtain system matrices which maintain a stable structure under a Galerkin projection.

Since the standard projection matrix can be used, the ROM size does not increase and there is no additional cost to preserving stability. For this reason the method using the $u-\phi$ formulation presented here is preferred over the method using the $u-p$ formulation from section 3.1.1.

3.2. Discrete-time state-space representation

The systems of ordinary differential equations in Eqs. (8) and (10) contain second-order time derivatives, while the Kalman filter described in Sec. 2 requires a first-order state space representation. This can be easily obtained by rearranging the equations of motion in first order form for the reduced order model as:

$$\begin{bmatrix} \dot{\mathbf{q}} \\ \ddot{\mathbf{q}} \end{bmatrix} = \begin{bmatrix} \mathbf{0} & \mathbf{I} \\ -\left(\mathbf{M}^r\right)^{-1}\mathbf{K}^r & -\left(\mathbf{M}^r\right)^{-1}\mathbf{C}^r \end{bmatrix} \begin{bmatrix} \mathbf{q} \\ \dot{\mathbf{q}} \end{bmatrix} + \begin{bmatrix} \mathbf{0} \\ \left(\mathbf{M}^r\right)^{-1}\mathbf{F}^r \end{bmatrix} \mathbf{b} + \begin{bmatrix} \mathbf{0} \\ \mathbf{s} \end{bmatrix} \tag{19}$$

$$\mathbf{h} = \begin{bmatrix} \mathbf{H}^{pos} & \mathbf{H}^{vel} \end{bmatrix} \begin{bmatrix} \mathbf{q} \\ \dot{\mathbf{q}} \end{bmatrix} + \mathbf{r}, \tag{20}$$

with $\mathbf{b} \in \mathbb{R}^{n_f}$ the time-dependent inputs to the system (containing both structural forces and acoustic volume sources) and $\mathbf{F}^r \in \mathbb{R}^{n_r \times n_f}$ a selection

matrix or load distribution matrix for the ROM. This matrix can be obtained from a matrix $\mathbf{F} \in \mathbb{R}^{n \times n_f}$ selecting the position where the external forces or acoustic volume sources act on the unreduced model as:

$$\mathbf{F}^r = \mathbf{V}^T \mathbf{F}. \tag{21}$$

These continuous-time state-space equations can be summarized as:

$$\begin{aligned} \dot{\mathbf{x}} &= \mathbf{A}^c \mathbf{x} + \mathbf{B}^c \mathbf{b} \\ \mathbf{h} &= \mathbf{H}\mathbf{x} + \mathbf{r} \end{aligned} \tag{22}$$

However, the classical Kalman filter, as described in Sec. 2, requires the model equations in discrete time-form. In order to convert this continuous-time model to discrete time a range of time-integrators can be employed. In this work we propose to use an exponential integrator for the time-discretization of the model with a zero-order hold approximation for the external input force:

$$\begin{bmatrix} \mathbf{A}^d & \mathbf{B}^d \\ \mathbf{0} & \mathbf{I} \end{bmatrix} = exp\left(\begin{bmatrix} \mathbf{A}^c & \mathbf{B}^c \\ \mathbf{0} & \mathbf{0} \end{bmatrix} \Delta t \right) \tag{23}$$

Computing the matrix exponential [**?**] is a numerically unstable operation for high-order models and can therefore not be reliably applied to the original finite-element model. However, the ROM used in the estimator is typically of sufficiently small size, such that the matrix exponential can be reliably computed. As this is an exact solution to the ordinary differential equations describing the evolution of the ROM, this approach also allows for large timesteps Δt. The timestep can therefore easily be synchronized with the sampling frequency of the input and output measurements.

In short, the finite element method is used to obtain a high-fidelity, three-dimensional numerical model of the studied vibro-acoustic system, and is established using either the $u-p$ or the $u-\phi$ formulation. From this a reduced-order model is developed using an appropriate stability-preserving model order reduction method. Finally the ROM is rewritten in state space form to make it fit for use in the Kalman filter.

4. Detectability, model formulation and sensor selection

The long term stability of the Kalman filter described in section 2 depends on the limit behaviour of the covariance matrix $\mathbf{P}$. For linear time invariant systems $\mathbf{P}$ should converge to a steady state value $\mathbf{P}_\infty$, and in turn the Kalman gain matrix $\mathbf{G}^k$ will also evolve to the steady state Kalman gain $\mathbf{G}^k_\infty$. The convergence of $\mathbf{P}$ implies that the uncertainty on the state estimates remains bounded. In case $\mathbf{P}$ does not converge, the uncertainty on the state estimate grows without bound and no relevant information can be retrieved from the Kalman filter. Since in this case also the Kalman gain $\mathbf{G}^k$ becomes unbounded, the filter may behave in an unstable manner.

In order to guarantee the existence of a steady state covariance and Kalman gain, thus ensuring the stability of the Kalman filter, it is sufficient for the matrix pair $(\mathbf{A}^c, \mathbf{H})$ to be detectable. Detectability is a slightly weaker requirement than observability: a system is detectable when all states are either observable or stable. Since the system matrix $\mathbf{A}^c$ cannot be directly altered without sacrificing model accuracy, possible detectability issues should be resolved by altering the measurement matrix $\mathbf{H}$. In practice this means

that sensor selection and placement ultimately determine the detectability of the system and hence the long term stability of the Kalman filter. The type of formulation ($u-p$ or $u-\phi$) that is used in the vibro-acoustic finite element model affects both the system matrix and the measurement matrix. It will therefore have an impact on the types of sensors that are required to obtain a fully detectable system.

An insightful tool for assessing the observability of the matrix pair $(\mathbf{A}^c, \mathbf{H})$ (with $\mathbf{A}^c \in \mathbb{C}^{n_r \times n_r}, \mathbf{H} \in \mathbb{C}^{n_m \times n_r}$) is the PBH criterion [10]. This states that the matrix pair $(\mathbf{A}^c, \mathbf{H})$ is observable if and only if the PBH matrix

$$\mathcal{O}^{PBH} = \begin{bmatrix} s\mathbf{I} - \mathbf{A}^c \\ \mathbf{H} \end{bmatrix} \tag{24}$$

is of full column rank for any $s \in \mathbb{C}$. Since $s\mathbf{I} - \mathbf{A}^c$ only becomes singular at the system eigenfrequencies, it suffices to merely investigate the observability of the system modes. When examining detectability instead of observability, this means that solely unstable modes cause problems when they are not observable. This can be checked for individual modes by evaluating the PBH matrix at the corresponding eigenfrequency.

The reduced-order vibro-acoustic models from section 3 are guaranteed to have their eigenvalues in the left-half of the complex plane. In the context of these vibro-acoustic systems, detectability problems can only occur in case of:

- *Undamped systems*: Since all modes are only marginally stable, any unobservable mode will lead to a non-detectable system and may cause

stability problems in the Kalman filter. However in almost all real-world applications a damping matrix will be present, making this a nonissue.

- *Rigid body modes*: These are modes with eigenfrequency 0, and will therefore lead to a non-detectable system if they are unobservable. The presence of a damping matrix has no influence on these rigid body modes.

The remainder of this paper assumes that some form of damping is present, such that only the problem of rigid body modes remains. For vibro-acoustic finite element models, the rigid body modes and their observability do not only depend on the available measurements, but also on the adopted finite element formulation. The following sections will study the effect of these rigid body modes on the detectability of the system for the model approaches proposed in this work.

4.1. Acoustic rigid body modes

$u-p$ formulation. In this paper we propose a virtual sensing method that solely relies microphone measurements. When using the $u-p$ formulation, the PBH matrix is then given by:

$$\mathcal{O}^{PBH,up} = \begin{bmatrix} s\mathbf{I} - \mathbf{A}^c \\ \begin{bmatrix} \mathbf{H}^{pos} & \mathbf{H}^{vel} \end{bmatrix} \end{bmatrix} = \begin{bmatrix} s\mathbf{I} - \mathbf{A}^c \\ \begin{bmatrix} \mathbf{0} & \mathbf{H}^{pres} & \mathbf{0} & \mathbf{0} \end{bmatrix} \end{bmatrix}, \tag{25}$$

where $\mathbf{H}^{pres}$ is a selection matrix for the microphone (pressure) measurements.

The acoustic field only has one rigid body mode, namely the variation of the equilibrium pressure level. When evaluating the PBH matrix at $s = 0$, the column rank of $\mathbf{A}^c$ is therefore $n_r - 1$. However, this rigid body mode is captured by the microphone measurements, and it is therefore observable. The system is fully detectable, and the Kalman filter will evolve to a steady state.

In practice microphones do not necessarily accurately capture the equilibrium pressure level, or very low frequency pressure variations for that matter. However, this equilibrium pressure level is usually of no interest for acoustic problems. The (inaccurately measured) DC component may therefore be filtered out of the measurement signals, technically fixing the measured equilibrium pressure arbitrarily to 0. Since the system is observable, this will effectively avoid any practical detectability problems and ensure Kalman filter stability.

$u - \phi$ formulation. In case the $u - \phi$ formulation is used to describe the vibro-acoustic system, not only the system matrix $\mathbf{A}^c$ is different, but also the measurement matrix $\mathbf{H}$ changes. With ϕ now as the primary variable and p depending on the time derivative thereof, the microphone measurements transforms from $\mathbf{H}_{pos}$ to $\mathbf{H}_{vel}$. This leads to the following PBH matrix:

$$\mathcal{O}^{PBH,u\phi} = \begin{bmatrix} s\mathbf{I} - \mathbf{A}^c \\ \begin{bmatrix} \mathbf{H}_{pos} & \mathbf{H}_{vel} \end{bmatrix} \end{bmatrix} = \begin{bmatrix} s\mathbf{I} - \mathbf{A}^c \\ \begin{bmatrix} \mathbf{0} & \mathbf{0} & \mathbf{0} & \mathbf{H}^{pres} \end{bmatrix} \end{bmatrix}. \tag{26}$$

The acoustic field now possesses two rigid body modes. The first rigid body mode is again the variation of the equilibrium pressure level, and the second

is the variation of the equilibrium velocity potential level. The microphone measurements are theoretically able to observe the equilibrium pressure level, but since $p = -\rho\dot{\phi}$ the equilibrium level of the velocity potential does not have any effect on the pressure and can therefore not be observed using microphone measurements. The system will be non-detectable as a consequence.

As a solution to this problem one could use so-called *dummy measurements* [11] to pin the velocity potential equilibrium level to an arbitrary value. Since this level has no influence whatsoever on the sound pressure nor the particle velocity, it is of little practical interest and will not show up in any physical or virtual measurements. It is therefore perfectly justifiable to use this dummy measurement approach to ensure the detectability of the system, which in turn leads to a stable Kalman filter implementation.

4.2. Structural rigid body modes

The structural part of the model, if present, may also contain rigid body modes. In some very particular cases the main acoustic rigid body mode (the equilibrium pressure variation) can be coupled to a structural rigid body mode, for example when the structure moves in a piston-like way in an enclosed space. In all other situations structural rigid body modes will not be perceptible in the acoustic pressure, and are therefore unobservable when solely relying on microphone measurements. In order to prevent Kalman filter instability it is therefore essential to either add position/displacement sensors to the set-up or to adopt the aforementioned technique of including dummy measurements.

4.3. Practical results and conclusions

The analysis in this section has shown that, under the assumption of real-world applications where a minimal amount of damping is present, microphone measurements are very well-suited to virtual sensing applications. The proposed technique of combining reduced-order finite element models with microphone measurements can be made to produce long-term stable Kalman filter based virtual sensors. Care has to be taken when the $u - \phi$ formulation is adopted, since a dummy measurement is required to remedy the unobservability of the additional rigid body mode [11]. The existence of structural rigid body modes also presents complications, but these can be resolved by adding displacement sensors or including dummy measurements.

5. Virtual sensor overview

The aim of the virtual sensor is to leverage a small number of real measurements through the numerical model of the system in order to obtain measurements which cannot be performed directly. In this particular work, the aim is to obtain virtual measurements for the full sound field in the region of interest from only a small number of actual microphone measurements. The full process for obtaining the virtual measurements, including the previously described steps, is summarized here:

- *Instrument system under test.* First the system under investigation has to be defined and instrumented. In this case the sensorization consists of mounting a limited number of microphones in the cavity under investigation. Depending on the application, these microphones can be mounted based on practicality or to maximize the observability of the

system [**?**]. One (or multiple) force cell(s) is also required to record the main excitation(s) to the structure. Providing these excitation measurement is relatively straightforward in a laboratory setting, but can prove to be an issue for in-the-field measurements.

- *Set up high-fidelity model.* A high-fidelity reference finite-element model needs to be set up for the system on which the measurements will be performed. Any of the two approaches proposed in Sec. 3 can be used. If some parameters of the system are unknown, a model updating procedure can first be performed based on the available reference measurements.

- *Perform model reduction.* Once the high-fidelity model is set up, a reduced order model can be constructed to use in the Kalman filter. First, an approach has to be chosen to construct the initial reduced order basis (ROB) for the ROM. A range of approaches have been discussed in literature with this aim [12, 13, 14, 15, 16, 17]. If the proposed $u - \phi$ formulation is used, this ROB can be directly used as $\mathbf{V}$. If the $u - p$ formulation is used, an additional splitting of the basis needs to be performed in order obtain the stability-preserving $\mathbf{V}$.

- *Perform state-estimation on sensor data.* In order to perform the state-estimation, the reduced order model is discretized in time, using the exponential integrator, and matching the timestep Δt to the sensor sampling frequency. Now the state-estimation can be performed through the Kalman filter, see Sec. 2, for the reduced state vector $\mathbf{q}$.

- *Transform to full field virtual measurement.* The state-estimation pro-

vides the states for the reduced model $\mathbf{q}$. However, in order to obtain the desired virtual microphone measurements, the data needs to be transformed back to the unreduced coordinates. If the original model is described in the $u-p$ formulation, the virtual microphone measurements are obtained as:

$$\mathbf{p} = \mathbf{V}_{up}\mathbf{q}. \tag{27}$$

If the original high-fidelity model is described in the $u-\phi$ formulation, the pressure distribution over the nodes is obtained as:

$$\mathbf{p} = -\rho\mathbf{V}_{u\phi}\dot{\mathbf{q}}. \tag{28}$$

If additional virtual measurement points are required, besides the nodal pressures, the finite-element shape functions can be exploited to evaluate additional locations as well.

These virtual measurements can then be used to perform a range of analyses, depending on the final purpose. As the virtual measurements are performed in time-domain, the generated data is useful for transient analysis, but can also be easily transformed into the frequency domain for further analysis.

6. Experimental validation

In this section the proposed virtual microphone sensing approach is validated experimentally, thereby demonstrating its performance in real-world applications.

6.1. Experimental set-up, instrumentation and modelling

The experimental set-up used for this validation is the KU Leuven SoundBox [18], as depicted in figure 1. This is a concrete cabin that encapsulates

Figure 1: The KU Leuven SoundBox test set-up.

a convex volume with non-parallel but planar rigid walls. The front of the cabin is sealed by a rigid steel frame containing an A2-sized opening. A flexible panel can be installed over the opening by using the two rows of bolts around it, using a specific mounting frame to effectively clamp the edges of the plate in place. The flexible panel and enclosed cavity constitute a strongly coupled vibro-acoustic system.

A 2mm thick aluminium panel is clamped to the front wall of the SoundBox for the experimental validation of the virtual microphone sensing method. The system is excited using a modal impact hammer that is equipped with a force transducer. The cabin is instrumented with six prepolarized condenser microphones as schematically shown in figure 2. Only four of these microphones (M1 - M4) are included as sensors for the Kalman filter, the other

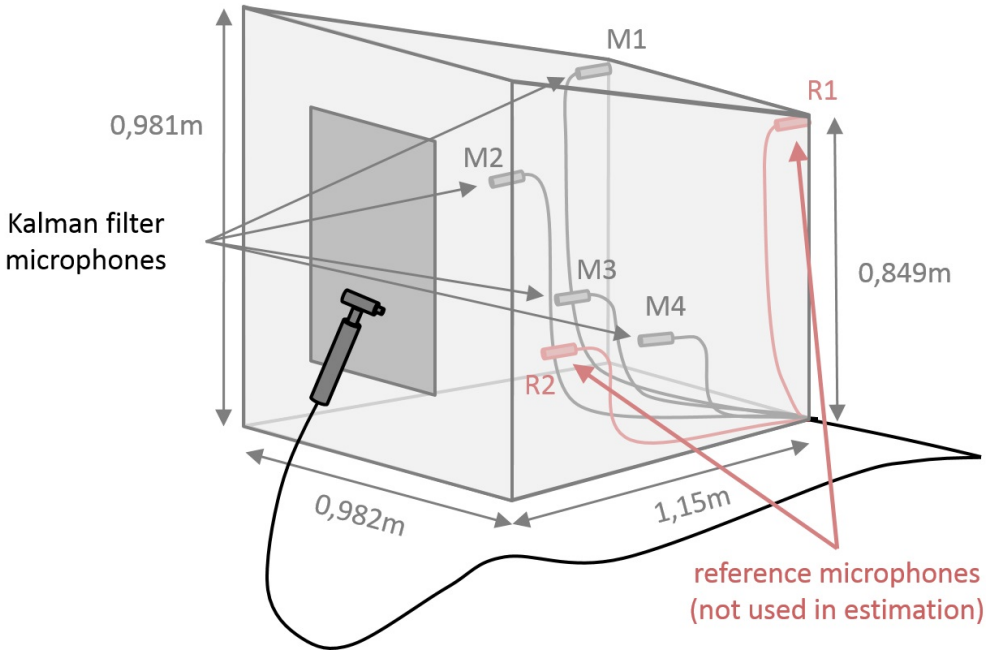

Figure 2: Schematic of the experimental set-up and instrumentation.

two microphones (R1 and R2) are used to provide reference data for the estimated states. These reference measurements serve to judge the accuracy of the virtual sensing approach.

The numerical model used in the Kalman filter assumes that the walls of the SoundBox are acoustically rigid, except for the flexible aluminium panel. The panel is considered to be clamped along its edges. The acoustic domain is discretized using tetrahedral elements with quadratic shape functions while the panel is modelled using shell elements, also with quadratic shape functions. The element size is chosen such that the spatial discretization is accurate up to 400 Hz [19], and the damping in the system is modelled as Rayleigh damping. The frequency response function characterizing the sound

pressure at the location of microphone R1 as a response to the force input by the modal hammer (both measured and simulated) is shown in figure 3.

The finite element model contains 22993 DOFs which makes it far too large

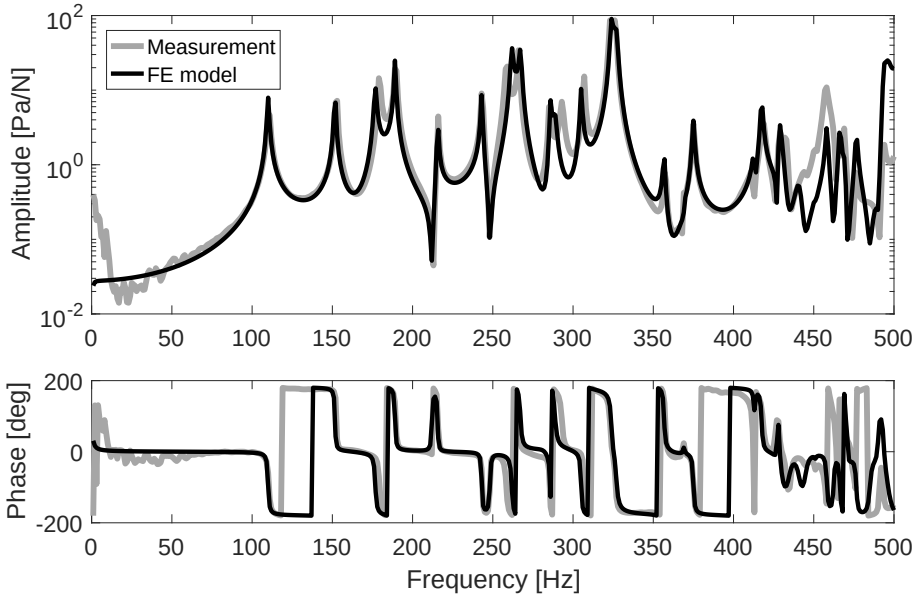

Figure 3: Experimental and numerical frequency response function of sound pressure over force for the location of microphone R1.

for direct use in the Kalman filter. The ROM is constructed using a Krylov subspace projection method [13]. The second-order Arnoldi (SOAR) method is used to construct the projection matrices [14]. In order to warrant the stability of the ROM, the system is established in the $u-\phi$ formulation discussed in section 3.1.2. The ROM only consists of 68 DOFs, while still providing a very accurate description of the system dynamics. The relative difference between the frequency response functions of the finite element model and the ROM is shown in figure 4 and is smaller than $2.5 \cdot 10^{-3}$ over the whole

frequency range of interest $(0 - 400$ Hz).

The continuous-time system was discretized using an exponential integrator

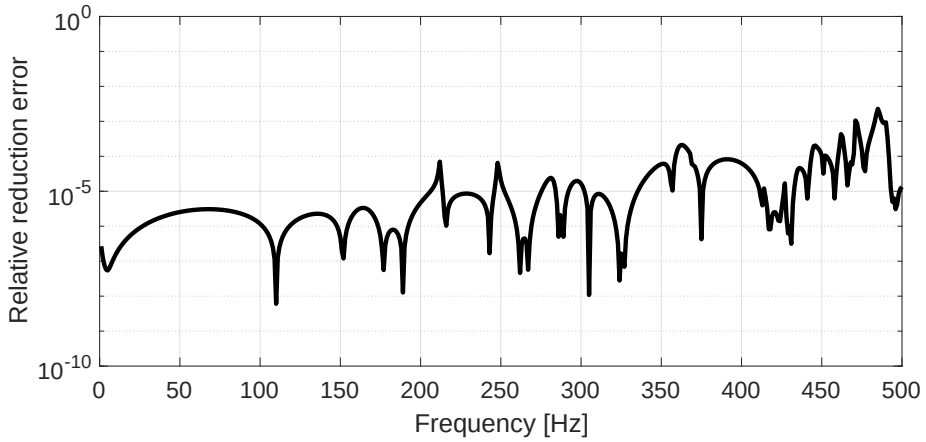

Figure 4: Relative reduction error for the location of microphone R1.

and a time-step size Δt that was matched to the sensor sample rate of 16384 Hz.

6.2. Virtual sensor performance

The Kalman filter estimates the full system state which facilitates virtual measurements at any desired field point. Technically this approach produces a virtual measurement of the entire sound field from only a very limited amount of physical sensor data (originating from the force cell and four microphones in this particular case). In order to characterize the accuracy of this approach, a reference pair of physical sound pressure measurements (which were not used in the virtual sensing algorithm) are compared to the virtual sound pressure measurements at the same locations. To illustrate the added value of the sound pressure measurements in the Kalman filter

approach, the proposed virtual sensing method is also compared to a direct simulation of the sound pressure starting from the experimentally measured force excitation.

Figures 5 and 6 show the comparison of the reference, virtual and simulated sound pressure levels at the location of microphones R1 and R2. The reference and virtual measurements are very closely matched, proving that the virtual sensing approach developed in this work is accurate and reliable in real-world conditions. The required computations can be performed *faster than real time* in MATLAB on a PC for the studied vibro-acoustic system. Additionally the figures illustrate that the Kalman filter performs much better than a direct simulation, indicating that it is necessary to include some form of feedback using measured physical quantities to construct an accurate virtual sensor. A direct simulation may produce acceptable results initially, but errors accumulate over time and the accuracy quickly diminishes. Figure 7 shows the reference, virtual and simulated sound pressure levels for microphone R2 after a second of acquisition time. While the simulation produces a completely inaccurate pressure estimate, the Kalman-based virtual sensor still closely matches the physical reference sensor signal.

Each physical sensor signal that is used in the Kalman filter carries useful information. Including additional physical measurements therefore typically improves the Kalman state estimate and hence also the accuracy of the virtual measurements. Figure 8 analyzes how the quality of the virtual measurements improves when the number of microphones that are used in

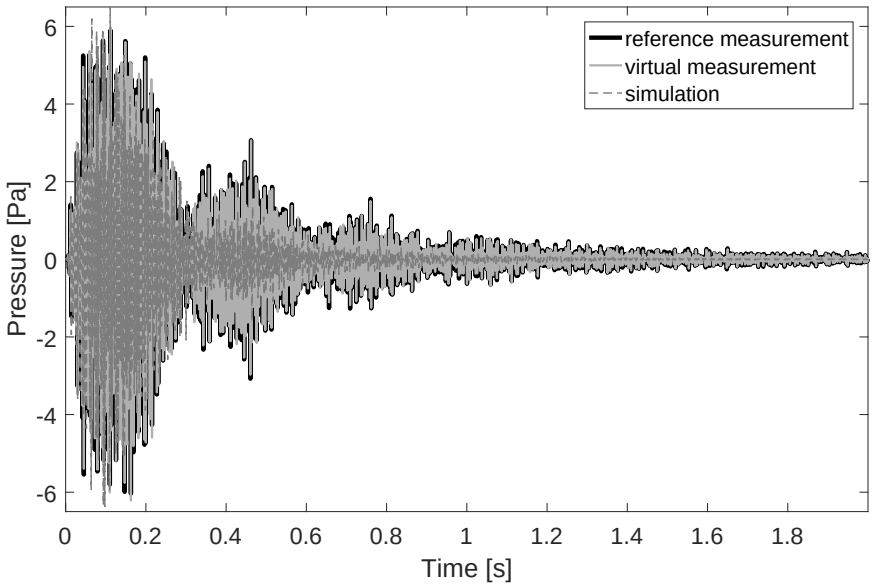

(a) Overview of the microphone R1 reference and virtual measurements.

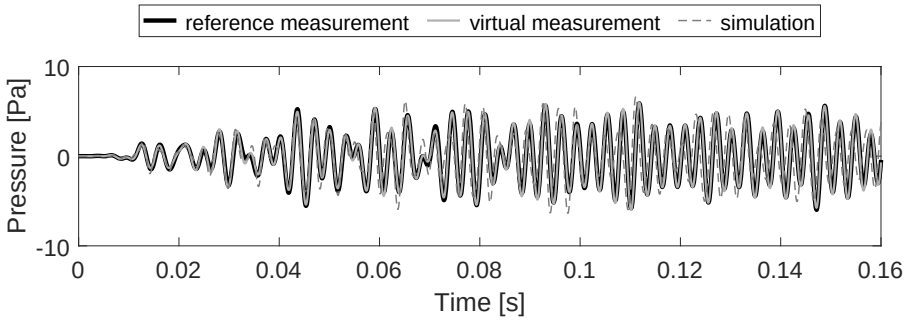

(b) Close-up of the microphone R1 reference and virtual measurements.

Figure 5: Reference and virtual measurements of microphone R1.

the Kalman filter increases. The accuracy of the virtual measurements is quantified using the error variance, which acts as a mean squared error and is defined as

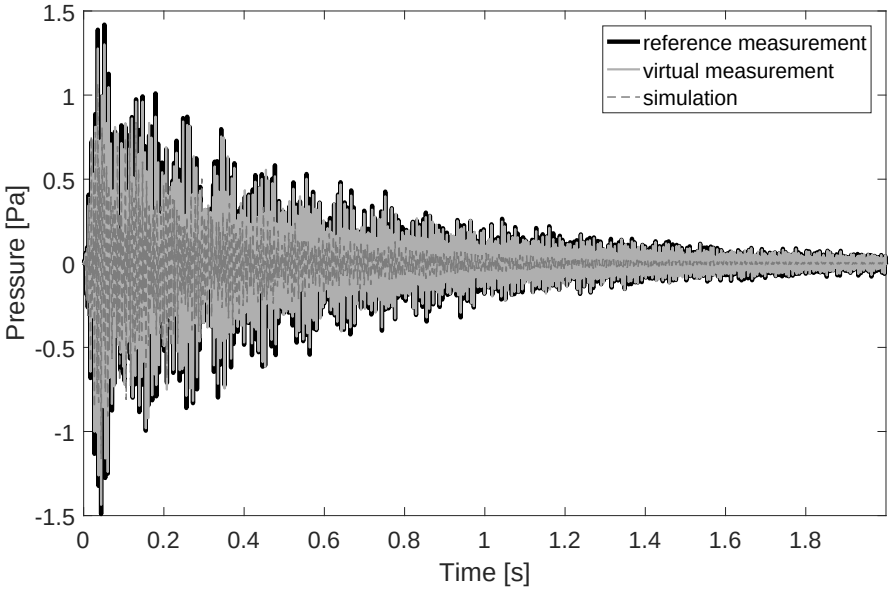

(a) Overview of the microphone R2 reference and virtual measurements.

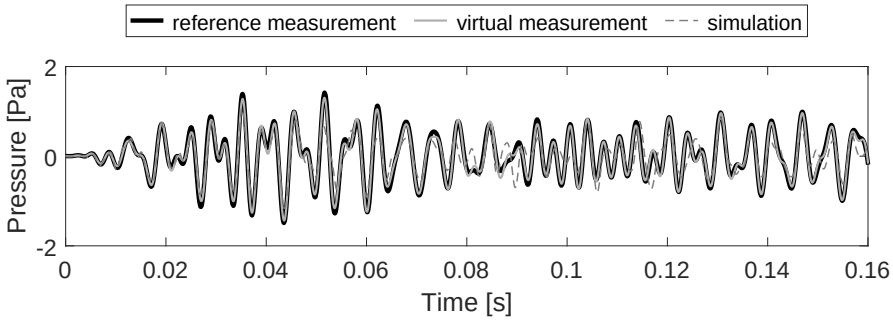

(b) Close-up of the microphone R2 reference and virtual measurements.

Figure 6: Reference and virtual measurements of microphone R2.

$$\varepsilon_{var} = \frac{\Sigma_{k=1}^{q} \left(p_{ref}(t_k) - p_{virt}(t_k)\right)^2}{n_s}, \tag{29}$$

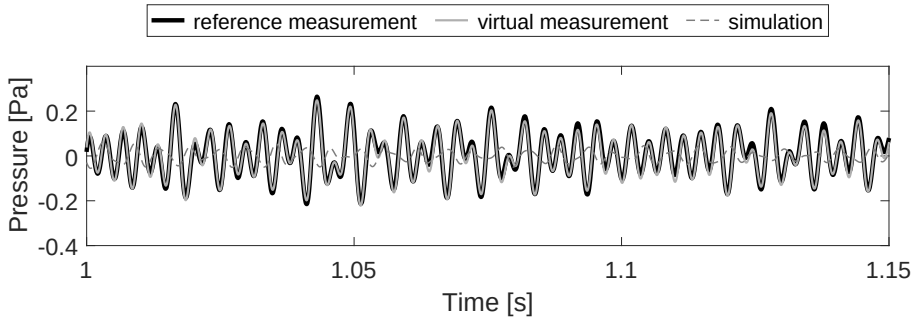

Figure 7: Error accumulation causes the simulation to lose accuracy over time, while the Kalman-based virtual sensor remains accurate.

where n_s is the total number of time steps in the analysis. Figure 8 indeed shows that this error variance decreases when more microphone measurements are included in the Kalman filter. This increase in virtual sensor accuracy is most prominent when moving from a direct simulation approach (0 microphones) to the Kalman filter approach with a single microphone measurement. The error variance further decreases when more microphones are added, but the rate of improvement declines.

The virtual sensor has been shown to perform well at the locations of the reference microphones R1 and R2. No specific assumptions were made with respect to the location of these reference microphones, and we can therefore assume that similar virtual sensor accuracy is reached at other locations. In fact switching reference microphones with the ones used in the Kalman filter produces comparable results at the other microphone locations. In contrast to physical microphones, the Kalman-based virtual sensor is able to measure the entire system state, and effictevly produces a virtual measurement of

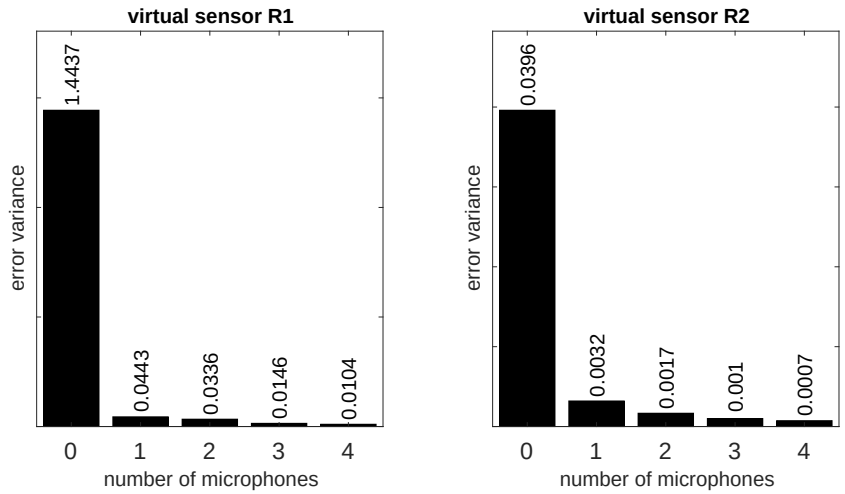

Figure 8: Evolution of the virtual sensor error variance with increasing number of microphones used in the Kalman filter.

the whole sound field. As an illustration figure 9 shows a snapshot of the virtually measured sound field.

7. Conclusion

This work proposes a virtual microphone sensing approach that merges physical microphone measurements with a numerical model in a Kalman filter. The developed virtual sensor is able to characterize the sound field at uninstrumented locations. As a result the proposed method grants the physical insight of a simulation but now with the real-world accuracy of an experimental measurement. The use of a finite element model, combined with efficient model order reduction techniques, ensures that the model used in the virtual sensor is accurate while remaining real-time capable, even for three-dimensional systems of realistic size and complexity. The proposed

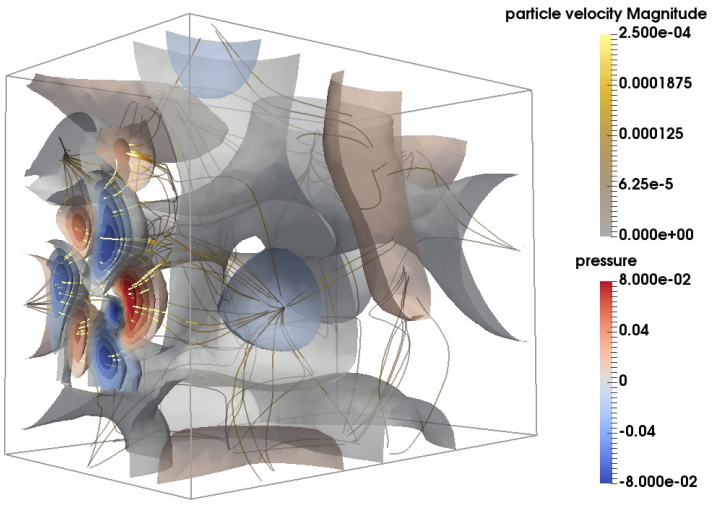

Figure 9: Snapshot of the virtually measured sound field at t = 0.036s. The isosurfaces indicate pressure levels while the streamlines depict the particle velocity.

method is shown to generate very accurate virtual sound measurements in a real test case.

Acknowledgements

The research of Frank Naets is funded by a Ph.D grant of the Institute for the Promotion of Innovation through Science and Technology in Flanders (IWT-Vlaanderen) and his research stay at LIM-UDC was funded by a grant from the Fund of Scientific Research (FWO).

References

[1] D. Moreau, B. Cazzolato, A. Zander, and C. Petersen. A review of virtual sensing algorithms for active noise control. *Algorithms*, 1:69–99, 2008.

[2] C.D. Petersen, A.C. Zander, B.S. Cazzolato, and C.H. Hansen. A moving zone of quiet for narrowband noise in a one-dimensional duct using virtual sensing. *The Journal of the Acoustical Society of America*, 121(3):1459–1470, 2007.

[3] C.D. Petersen, R. Fraanje, B.S. Cazzolato, A.C. Zander, and C.H. Hansen. A kalman filter approach to virtual sensing for active noise control. *Mechanical Systems and Signal Processing*, 22(2):490–508, 2008.

[4] D. Halim and Z. Cheng, L. andSu. Virtual sensors for active noise control in acoustic-structural coupled enclosures using structural sensing: Robust virtual sensor design. *The Journal of the Acoustical Society of America*, 129(3):1390–1399, 2011.

[5] D. Halim and Z. Cheng, L. andSu. Virtual sensors for active noise control in acoustic-structural coupled enclosures using structural sensing: Part ii - optimization of structural sensor placement. *The Journal of the Acoustical Society of America*, 129(4):1991–2004, 2011.

[6] F. Fahy. *Sound and Structural Vibration: Radiation, Transmission and Response*. Academic Press, London, 1985.

[7] R.E. Kalman. A new approach to linear filtering and prediction problems. *Journal of Basic Engineering*, 82(1):35–45, 1960.

[8] A. van de Walle, F. Naets, E. Deckers, and W. Desmet. Stability-preserving model order reduction for time-domain simulation of vibro-acoustic fe models. *International Journal for Numerical Methods in Engineering*, 109(6):889–912, 2017.

[9] G.C. Everstine. A symmetric potential formulation for fluid-structure interaction. letter to the editor. *Journal of Sound and Vibration*, 79(1):157–160, 1981.

[10] M.L.J. Hautus. Controllability and observability condition of linear autonomous systems. *Ned. Akad. Wetenschappen, Proc. Ser. A*, 72:443–448, 1969.

[11] F. Naets, J. Cuadrado, and W. Desmet. Stable force identification in structural dynamics using kalman filtering and dummy-measurements. *Mechanical Systems and Signal Processing*, 50:235–248, 2015.

[12] P. Benner, V. Mehrmann, and D. Sorensen, editors. *Dimension Reduction of Large-Scale Systems*. Springer Verlag, Berlin / Heidelberg, 2005.

[13] E.J. Grimme. *Krylov projection methods for model reduction*. PhD thesis, ECE Department, University of Illinois, 1997.

[14] Z. Bai and Y. Su. Dimension reduction of large-scale second-order dynamical systems via a second-order arnoldi method. *SIAM J. Scientific Computing*, 26:1692–1709, 2005.

[15] S. Gugercin and A.C. Antoulas. A survey of model reduction by balanced truncation and some new results. *International Journal of Control*, 77:748–766, 2004.

[16] R.R. Craig Jr., editor. *Structural dynamics: an introduction to computer methods*. John Wiley & Sons Inc, New York, 1981.

[17] B. Besselink, U. Tabak, A. Lutowska, N. van de Wouw, H. Nijmeijer, D.J. Rixen, M.E. Hochstenbach, and W.H.A. Schilders. A comparison of model reduction techniques from structural dynamics, numerical mathematics and systems and control. *Journal of Sound and Vibration*, 332(19):4403–4422, 2013.

[18] M. Vivolo. *Vibro-acoustic characterization of lightweight panels by using a small cabin*. PhD thesis, KU Leuven, Leuven, 2013.

[19] S. Marburg. Six boundary elements per wavelength: is that enough? *Journal of Computational Acoustics*, 10:25–51, 2002.